J|A|C|S
ARTICLES
Published on Web 09/18/2004

# Slow Motion, Trapping, and Sorting of Water- and Chloroform-Soluble Porphyrins in Nanowells

Sheshanath Bhosale,[†] Sidhanath Bhosale,[†] Tianyu Wang,[†] Guangtao Li,[‡] Ulrich Siggel,[§] and Jürgen-Hinrich Fuhrhop*[,†]

*Contribution from the Freie Universität Berlin, Institut für Organische Chemie, Takustrasse 3, D-14195 Berlin, Germany, Key Lab of Organic Optoelectronics and Molecular Engineering, Department of Chemistry, Tsinghua University, Beijing 10008, China, and Max-Volmer Institut für physikalische Chemie, Technischen Universität Berlin, Strasse des 17. Juni 135, D-10623 Berlin, Germany*

Received March 24, 2004; E-mail: fuhrhop@chemie.fu-berlin.de

***Abstract:*** A two-step self-assembly procedure on smooth, aminated silica particles established holey monolayers. At first, single, flat-lying porphyrin tetraamides (**A**) were bound covalently, followed by the build-up of a rigid monolayer made of diamido bolaamphiphiles (bolas) around the porphyrin islands. "Nanowells" around porphyrin (**A**) bottoms with a uniform diameter of 2.2 nm and varying depths of 0.6, 1.0, or 1.5 nm depending on the length of the applied bolas were thus obtained. Oligoethylene headgroups solubilized the particles in water, ethanol, and chloroform/ethanol, and two hydrogen bond chains between the secondary amide groups prevented swelling of the monolayer. Manganese(III) porphyrinates (**B**) migrated from the bulk solution to the bottom of the form-stable nanowells with a speed of about 1 pm/s and were trapped there above porphyrin (**A**). After isolation of the (**A**,**B**) particles by centrifugation or ultrafiltration, the particles were suspended in a chloroform solution of a chlorin (**C**), which was also fixated irreversibly on the bottom of the nanowells. The nanowells thus contained three different porphyrins **A**,**B**,**C** in a noncovalent stack. The reverse sequence **A**,**C**,**B** was built-up correspondingly, first in chloroform/ethanol, and then in water. The "sorting" of **A**,**B**,**C** and **A**,**C**,**B** systems was characterized by visible spectra, sequence-dependent fluorescence quenching, and cyclic voltammetry of the top component. The molecular sorting method is the first of its kind and should be generally useful for the production of noncovalent reaction systems on any smooth surface.

## Introduction

"Nanowells" were constructed by a two-step self-assembly procedure: single, flat-lying porphyrin molecules were first attached covalently to the amine surface of smooth silica particles, and a rigid wall of a diamido bolaamphiphiles was then built around these molecular islands. In contact with water or solvents, the gaps were filled with the fluid without changing their volume and shape. The form stability of the container leads to the name "well"; the diameter of its porphyrin bottom, which varies from 1 to 3 nm, makes it a "nanowell". Such nanowells have been studied on gold electrodes by cyclic voltammetry and fluorescence quenching[1−3] and on gold[4,5] and silica[6,7] colloidal particles by spectroscopic methods only. The colloidal carrier of choice consists of smooth amine-coated silicagel particles with a diameter of 100 nm and no pores, such as that introduced by van Blaaderen.[7] Their modestly curved, reactive, and photochemically inactive surface provides a perfect basis for the establishment of a closed monolayer with nanowells. As a most versatile headgroup, oligoethylene was selected, which renders the particles well-soluble in both water and many organic solvents. So far, we have studied these particles only in water.[6] It will be shown here that the nanowells are also form-stable in ethanol or chloroform. No swelling of the walls occurs, and porphyrins, which have the same size as the bottom porphyrin, enter the nanowells freely and are fixated slowly and irreversibly on its ground. On the basis of these findings, a sorting procedure for molecular stacks of hydrophilic and hydrophobic molecules in any order has been established for the first time.

In the following, we only exploit the irreversible entrapment of porphyrin-type dyes, because their presence and quantity can be established by spectroscopy of the Soret bands at 400 nm (chlorin), 420 nm (tetraphenylporphyrins), and 450 nm (manganese(III) porphyrinates) or the chlorin band at 650 nm. Time-dependent measurements of fluorescence quenching then es-

[†] Institut für Organische Chemie.
[‡] Tsinghua University.
[§] Technischen Universität Berlin.

(1) Fudickar, W.; Zimmermann, J.; Ruhlmann, L.; Roeder, B.; Siggel, U.; Fuhrhop, J.-H. *J. Am. Chem. Soc.* **1999**, *121*, 9539−9545.
(2) Skupin, M.; Li, G.; Fudickar, W.; Zimmermann, J.; Roeder, B.; Fuhrhop, J.-H. *J. Am. Chem. Soc.* **2001**, *123*, 3454−3461.
(3) Li, G.; Fudickar, W.; Skupin, M.; Klyszcz, A.; Draeger, C.; Lauer, M.; Fuhrhop, J.-H. *Angew. Chem., Int. Ed.* **2002**, *41*, 1828−1852.
(4) Li, G.; Doblhofer, K.; Fuhrhop, J.-H. *Angew. Chem.* **2002**, *114*, 2855; *Angew. Chem., Int. Ed.* **2002**, *41*, 2730−2734.
(5) Li, G.; Fuhrhop, J.-H. *Langmuir* **2002**, *18*, 7740−7747.
(6) Li, G.; Bhosale, S. V.; Wang, T.; Hackbarth, S.; Roeder, B.; Siggel, U.; Fuhrhop, J.-H. *J. Am. Chem. Soc.* **2003**, *125*, 10693−10702.
(7) von Blaaderen, A.; Vrij, A. *J. Colloid Interface Sci.* **1993**, *156*, 1−18.

10.1021/ja048310v CCC: $27.50 

tablish the speed of the porphyrin fixation within the wells and the sequence in ordered porphyrin stacks. Cyclic voltammetry will finally identify the outermost porphyrin and thereby also characterize the success of sorting.

## Experimental Section

**Synthesis.** Porphyrins **1**, **3**,[1−6] and **4**[8] have been described earlier. Bolaamphiphile (**2c**) 17-({2-[2-(2-methoxy-ethoxy)-ethoxy] ethoxy-methyl}-carbamoyl-)-heptadec-16-enoyl chloride was synthesized starting from 16-oxo-hexadecanoic-acid using the procedure as described for **5b** in ref 6. Aminated silica particles and the establishment of nanowells by two consecutive self-assembly steps were also described.[6,7]

**UV/Vis Spectroscopy of Silica Colloids.** UV/vis absorption spectra of membrane-coated silica colloids were acquired using a Perkin-Elmer Lambda 16 spectrometer.

**Construction of Nanowells with Porphyrin-Covered Silica Particles.** Silica particles with form-stable nanowells were prepared as described in our previous work.[6] The self-assembly time for porphyrin **1a** was limited to 2 h, and the concentration of the porphyrin was $10^{-4}$ M. For more details, see the sorting procedure below.

**Time-Dependent Fluorescence Quenching Experiments.** Fluorescence measurements and time-dependent quenching experiments were performed on a Perkin-Elmer spectrometer (LS50B). First, 3 mg of the silicate colloids coated with nanowells was dispersed in 3 mL of water, ethanol, and chloroform in a quartz cuvette. Next, 200 $\mu$L of an aqueous solution of the quencher such as Mn(III)-*meso*-tetra(3-methyl-pyridinium)-porphyrinate chloride **3b** in water ($10^{-4}$ M) or ethanol ($10^{-4}$ M), or of Mn(III)-*meso*-(tetraphenyl)porphyrinate chloride **1e** in $CHCl_3$ ($10^{-4}$ M), was added to a solution stirred with a pipet. The fluorescence intensity of the bottom porphyrin at 650 nm was then measured over periods between 1 and 24 h (Figure 1).

**Sorting of Three Porphyrins in the Nanowells.** To separate loaded particles from solutes in bulk solution, we used either centrifugation of ultrafiltration. Centrifugation was used when the upper porphyrin was relatively large, for example, a *para*-tetra(phenylsulfonato)-porphyrin **1d**. Smaller porphyrins, for example, chlorin **4**, were, however, partly removed from the nanowell by centrifugation. If they were added last, it was therefore necessary to apply an ultrafiltration procedure using a combination of a high-tensile steel frit in a short HPLC steel tubing with 100 nm pores (Duratec, Hockenheim, Germany) and a cellulose ultrafilter (Millipore) with 200 nm pores. Ultrafilters with smaller pores and which could be used with organic solvents were not available.

Aminated silica particles should have a density similar to that of quartz ($g$ = 2.7 g/cm$^3$). Each particle has an average diameter of 100 nm corresponding to a volume of $(\pi/6)d^3 = 0.5 \times 10^6$ nm$^3$ and a weight of $0.5 \times 10^6 \times 10^{-21} \times 2.7 \times 10^3$ mg $= 1.4 \times 10^{-12}$ mg and a surface area of $\pi d^2$ or 31 000 nm$^2$. The procedure to load the aminated silica particles with porphyrin **1a** to produce particle **1b** was as follows: 30 mg of aminated silica particles ($=2.1 \times 10^{13}$ particles with a total surface of $6.5 \times 10^{17}$ nm$^2$) was suspended in 0.5 mL of a $10^{-4}$ M solution of the anhydride **1a** in dichloromethane ($=3 \times 10^{20}$ porphyrin molecules) and was left standing for 2 h. If one considers the minimal area of a tetraphenylporphyrin with 4 nm$^2$, then $1.6 \times 10^{17}$ molecules could be bound to the amino surface of these 3.0 mg of silica particles. The solution provided a 200-fold excess. The bola acid chloride (**2a**, **b**, or **c**) in $CH_2Cl_2$ was then added (0.5 mL; $10^{-3}$ M), and the mixture was stirred overnight. The particles were centrifuged (4000 rpm) and washed three times with $CH_2Cl_2$, ultrasonicated for 1 min, and again centrifuged. The last supernatant was nonfluorescent. Next, 3.0 mg of the particles with a surface of $6.5 \times 10^{16}$ nm$^2$ or a maximum of $1.6 \times 10^{16}$ adsorbed porphyrin molecules in a flat-lying orientation was redissolved in 3.0 mL of chloroform or water. They showed absorption bands with an optical density corresponding always approximately to

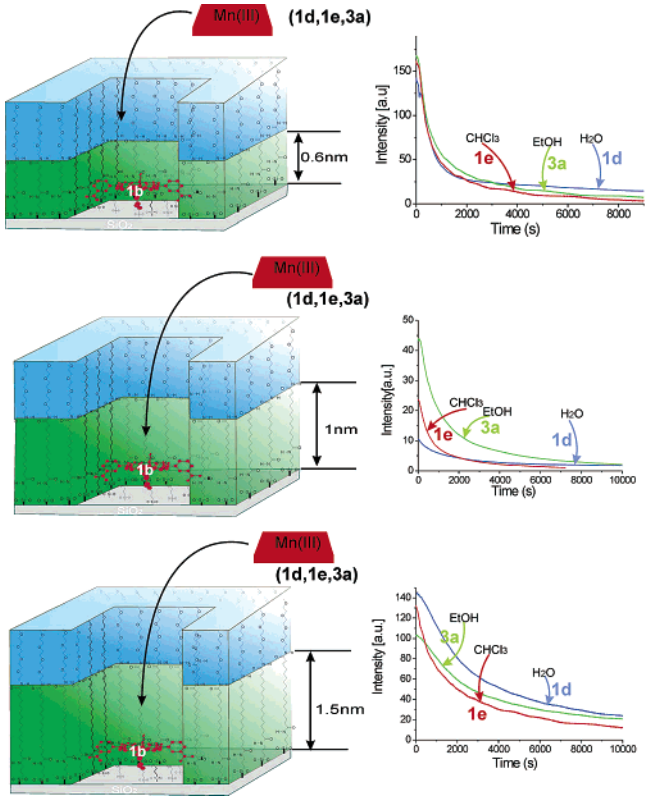


***Figure 1.*** Models of the 6, 10, and 15 Å wells, the entering porphyrin molecules, and quenching of the bottom porphyrin fluorescence by manganese(III) porphyrinate. **1d** and **3a** were applied in water, and **1e** was applied in chloroform. Also shown are the decay curves of the fluorescence of the bottom porphyrin after addition of different manganese porphyrins for the three nanowells.

$(3-4) \times 10^{-7}$ M solutions or $(5-6) \times 10^{14}$ porphyrin molecules or nanowells. These numbers were evaluated individually with an error of ±5% for each experiment. The percentage of porphyrin-covered silica was thus about 3−4%; 96−97% of the particle surface was then covered by the bola walls. About 3 mg of these particles was weighed, and 200 $\mu$L of a $10^{-4}$ M porphyrin or chlorin solution was added ($=1.2 \times 10^{16}$ porphyrin molecules). This number is about 20 times higher than that of the nanowells; about 5% of the molecules were trapped by the nanowells. The rest may be largely adsorbed to the extended OEG-surface of the particles and was washed off in the three cleaning cycles after each loading. The 20-fold excess was found to be a minimum for total quenching. A larger excess was avoided, because we did not want to fill up the nanowells with one type of porphyrin molecule only. The loading with chlorin **4** was undertaken in chloroform/ethanol = 10:1 to dissolve the chlorin and suspend the particles efficiently. First, 3.1 mg of the particles was suspended and then 200 $\mu$L of the $10^{-4}$ M chlorin **4** solution was added. The solution was left standing for 1 h and then filled with some pressure from the syringe into a short steel HPLC column with a 200 nm cellobiose ultrafilter and a 100 nm steel frit (Duratec, Hockenheim, Germany). The filtrate appeared as a clear solution. The cellobiose filter was then dropped into water or chloroform depending on its further progressing. Solution and filter were shortly and mildly sonicated, and the solution was decanted and filled up to 3.0 mL. UV/vis and fluorescence spectra were measured, and 200 $\mu$L of the next porphyrin solution ($10^{-4}$ M) was added. Another filtration or a centrifugation procedure followed. Each filtration and redispersion procedure was accompanied by a loss of 10−20% of the particles; each centrifugation and redispersion procedure was accompanied by a loss of about 5−10%.

**Electrochemical Characterization of Nanowell-Modified Silica Particles.** First, 100 mg of dry silica particles was dispersed in 1 mL

(8) Brückner, Ch.; Dolphin, D. *Tetrahedron Lett.* **1995**, *36*, 3295−3298.

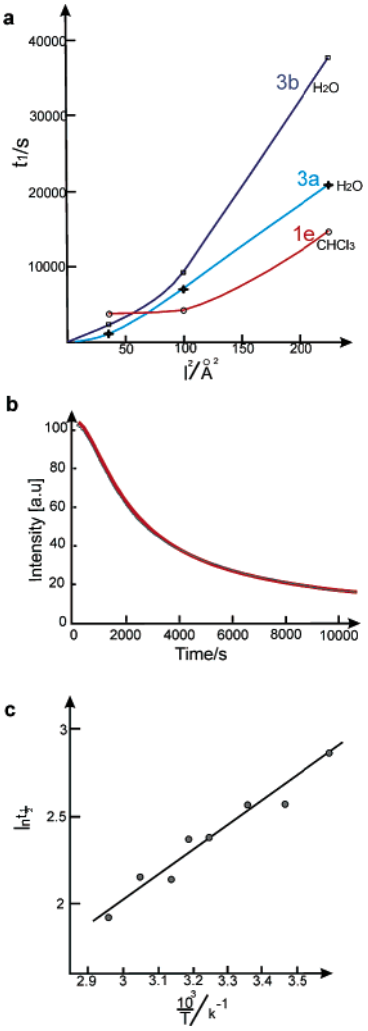


***Figure 2.*** Analysis of the time-dependence of fluorescence quenching by fitting a molecule in the nanowells: (a) the dependence of time-constant $t_1$ on nanowell depths for porphyrin **3a** (in $H_2O$), **3b** (in $H_2O$), and **1e** in ($CHCl_3$), (b) experimental (black) and calculated (red) curves fitted with eq 1 and one time-constant (15 Å nanowell, porphyrin **3a** in water), and (c) temperature-dependence of the half-time of the fast phase for porphyrin **3b** in water and nanowells of 10 Å depth.

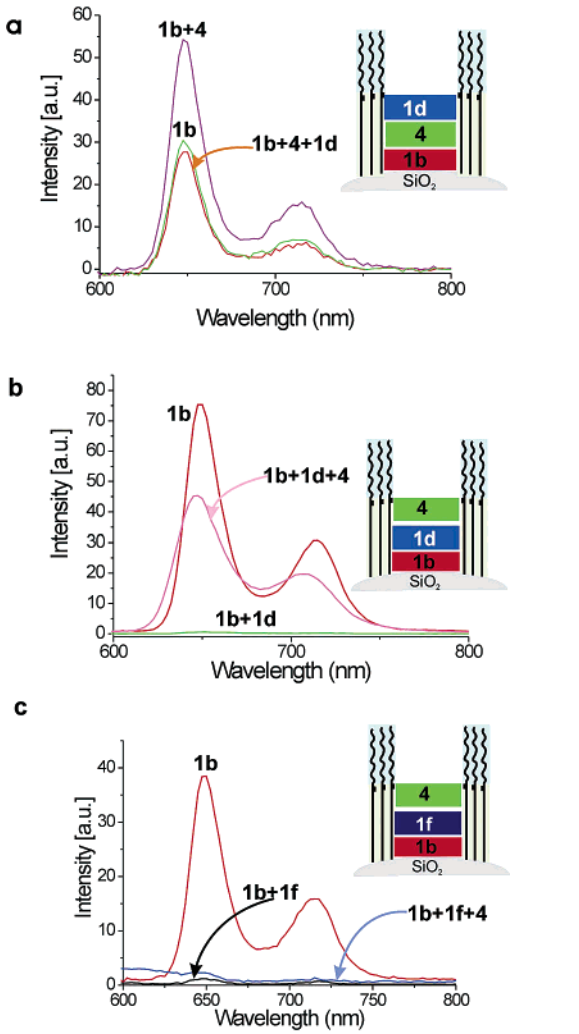


***Figure 3.*** Fluorescence of the silica particles (excitation at 420 nm, where products of absorption and quantum yield were found to be about equal for **4** and **1b**) containing only the bottom porphyrin **1b** (green trace), **1b** and chlorin **4** (violet), and **1b**, **4**, and manganese(III) porphyrin **1d** (red). The manganese(III) porphyrin quenches only the fluorescence of chlorin **4**, but not that of the bottom porphyrin. (b) The same experiment in the ordering **1b**, **1d**, **4**. The manganese(III) porphyrinate in the center of the sandwich quenches the fluorescence of the bottom porphyrin. The chlorin at the top is, however, separated by the chlorine counterion, and its fluorescence is not quenched significantly. (c) The same experiments with the copper(II)-porphyrinate **1f** without an axial counterion. If **1f** is in the center, it quenches the fluorescence of both the upper and the lower dye, quantitatively (violet trace).

of ethyl acetate. After a short sonification (10 s), a small amount of silver paste solution was added. The resulting mixture was spun on ITO or gold electrodes by spin coating and was dried in air (24 h) for electrochemical measurements. Cyclic voltammogram (CV) was performed in a 0.1 M $CH_2Cl_2$ solution of $TBAPF_6$ using a potentiostate PG310 (HEKA) operated with an IBM-compatible PC in a one-compartment three-electrode cell. Particle-modified ITO or gold electrodes (0.5 $cm^2$) were used as the working electrode. The counter electrode was a Pt wire, and Ag/AgCl was chosen as the reference electrode. For electrochemical characterization of the monomer, a platinum disk electrode (0.16 $cm^2$) was employed as the working electrode. Particles with redox-inactive porphyrins on top, naked silica particle, as well as the particle without any cover molecule were used for control experiments. An irreversible reduction wave for Mn(III) → Mn(II) was found only when the Mn(III) porphyrin was on top of the nanowells (see Figure 5).

## Results

The porphyrins **1a**−**f** and **3a**,**b**, the dioxychlorin **4**, and the bolaamphiphiles **2a**−**f** were synthesized by literature procedures as indicated in the Experimental Section (Scheme 1).

*meso*-Tetra(phenyl-3-carboxylate)-porphyrin **1a** was fixated covalently on amino-silicate particles to yield **1b** (**A**). The porphyrin was then surrounded with lipids **2a**−**c** in a second self-assembly step.[6] Nanowells with hydrophobic walls of three different heights, 6, 10, and 15 Å, were thus obtained on the particles' surface (Scheme 1; Figure 1). Semiquantitative estimates of the porphyrin concentration and the silica surface indicated that about 4% of the particles' surface was covered with porphyrins, and the other 96% was covered with rigid lipid walls (see Experimental Section). Because the surface of the particles was covered with oligoethylene groups, they were soluble in water as well as in chloroform or ethanol. The nanowells could thus be filled with any of these solvents, and corresponding solutes could be introduced. It was, however, not

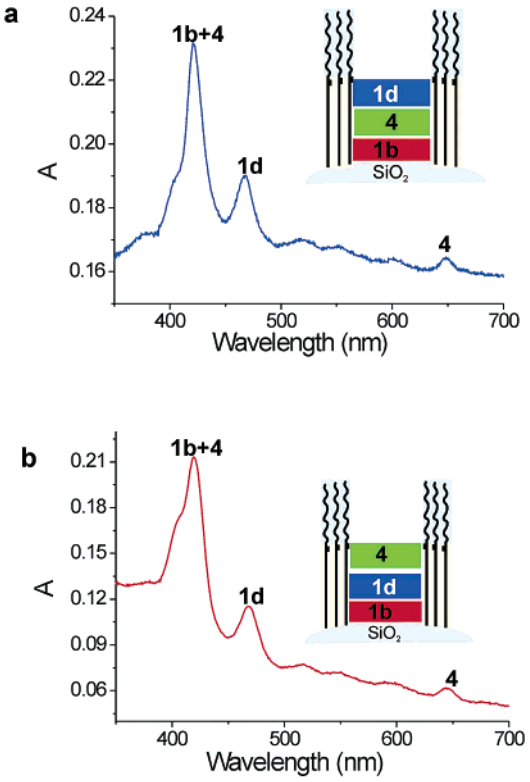


***Figure 4.*** The observed UV/vis spectra of (a) **1b**,**4**,**1d** (ratio of $10^{-7}$ molar concentrations: 1.9:1.75:2.2) and (b) **1b**,**1d**,**4** (ratio: 3.6:3.1:3.4) indicate a constant ratio of 1:1:1 with approximate errors of ±10%.

clear whether the lipid walls of the nanowells would swell or not swell in the organic solvents. We therefore checked the nanowells' form-stability. The particles were first dissolved in chloroform/ethanol 5:1 (v/v) and titrated with a chloroform solution of manganese(III)-tetra(phenyl-2-pyridinyl)porphyrinate **1c**. The diameter of this porphyrin is 3.6 nm, which is larger than the diagonal of the nanowell (2.8 nm) and therefore cannot enter it. It caused, nevertheless, a quenching of 5−10%, which probably indicates a few domains containing two or more neighboring porphyrin molecules on the bottom of larger nanowells. Titrations with the fitting porphyrins **1d**,**f** and **3a**,**b** in water and **1e** in chloroform, on the other hand, caused quantitative quenching. The half-time of this quenching process was extremely long (~$10^3$ s). These observations clearly indicate that the nanowells are form-stable in water, ethanol, and chloroform. Manganese(III) porphyrinates **1d** and **3a**,**b** were then added in water or in ethanol solution, manganese(III) tetraphenylporphyrinate **1e** was added in chloroform solution, and the decrease of the bottom porphyrin's fluorescence peak at 650 nm was measured with time. After a short time lag of about 5 s, which was caused by the slow response of the spectrometer, a nonexponential, in some cases sigmoidal, decrease was observed for all three nanowells and all three solvents (Figure 1).

The kinetics of the migration and the settlement of fitting manganese porphyrins on the bottom of the nanowells occur extremely slow. The pathway of 1−2 nm is so short that one can hardly find an analogy in normal diffusion processes. Furthermore, each well with a volume of about 10 $nm^3$ contains one porphyrin molecule at the end. The trapped porphyrin is

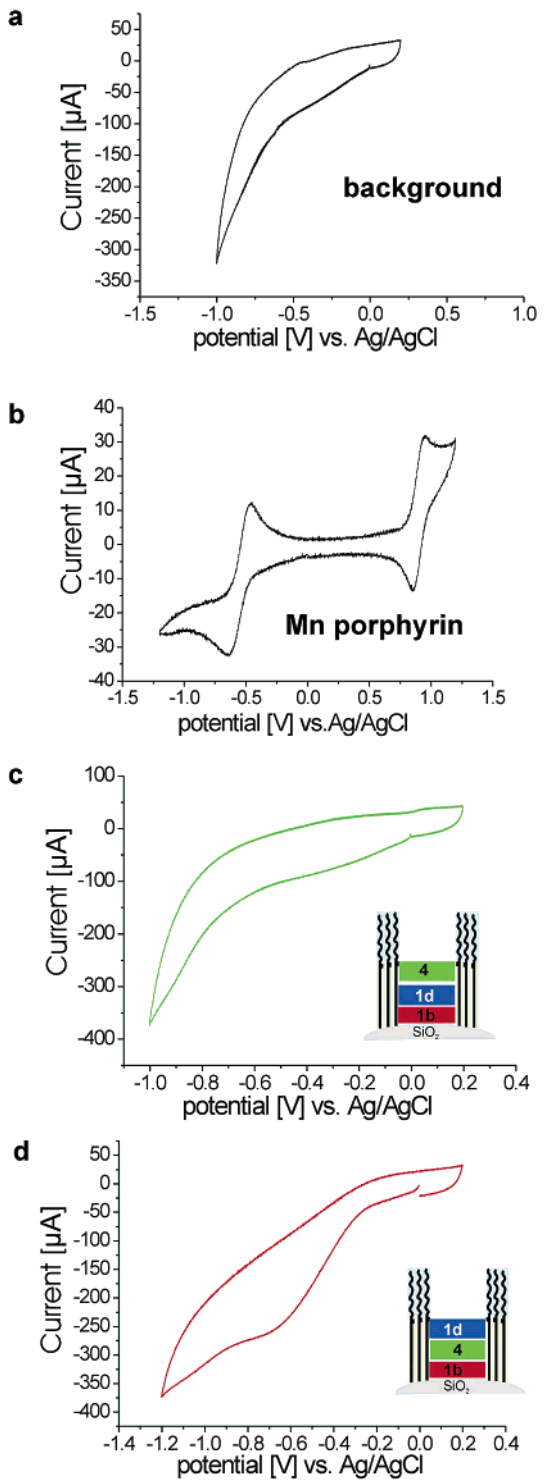


***Figure 5.*** Cyclic voltammograms of (a) the silver colloid without particles, (b) porphyrin **3a** in $CHCl_3$ solution, (c) silica particles with nanowells filled with porphyrins in the order **1b** → **3a** → **4** or **ABC**, and (d) silica particles with nanowells filled with porphyrins in the order **1b** → **4** → **3a** or **ACB**. Only (d) shows a peak for a manganese(III) reduction.

thus highly enriched in the nanowells in comparison to the bulk solution. We nevertheless tried to extract the approximate time and diffusion constants from the curves shown in Figure 1 by applying Fick's second law together with the Stern−Volmer equation for fluorescence intensity quenching, because we wanted to establish a time-constant and did not find more

***Scheme 1***

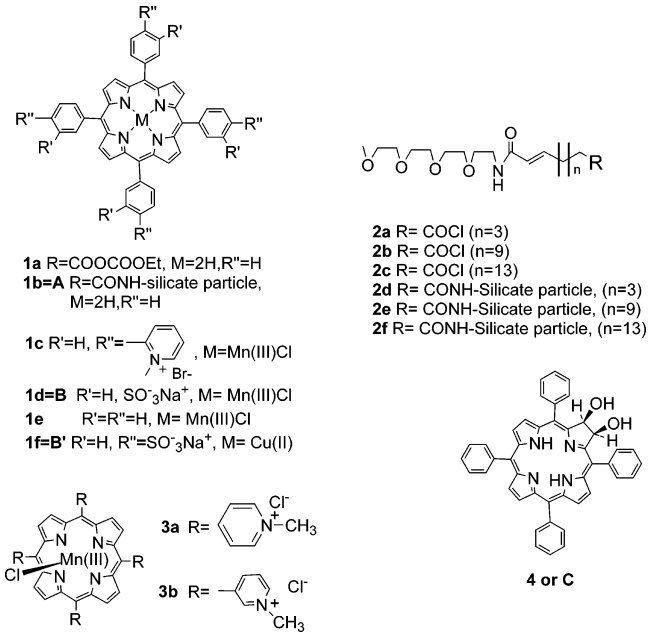


appropriate models. The result was eq 1 (see Supporting Information), which contains only one time-constant $t_1$.

$$\frac{F(t)}{F_0} = \frac{1}{1 + K_q[c_0 - \sum_n f_n \times e^{-(n^2\pi^2/l^2)Dt}]} \quad (1)$$

$$t_1 = \frac{l^2}{\pi^2 D} \quad (2)$$

Many of the curves of Figure 1 could be fitted surprisingly well with eq 1 and time-constants between 1300 and 3700 s. The sigmoid decay (Figure 2a) in the case of the 1.5 nm deep wells and water-soluble porphyrins was, for example, perfectly reproduced. Equation 2, which is analogous to that of Einstein−Smoluchowski, formulates a square dependence of the time-constant $t_1$ on the depth $l$ of the wells, which is approximately met particularly well for water-soluble porphyrins (Figure 2b). The $D$ values also responded to minor changes of the diameter of the quencher molecules. It was, for example, larger for the *meta*-methylpyridinium isomer **3b** by a factor of 2 as compared to the larger *para*-isomer **3a**. The viscosity of the solvent also played a role ($D_{CHCl_3} > D_{EtOH} > D_{H_2O}$; compare Figure 1). Temperature-dependent time curves could be separated into a fast and a slow phase with different amplitude ratios at different temperatures. The half-time of the fast phase followed an Arrhenius function with an activation energy of 2.7 kcal (Figure 2c).

We then took advantage of the slow and irreversible adsorption process to develop a procedure for the "sorting" of noncovalent porphyrin stacks in the orders **A**,**B**,**C** and **A**,**C**,**B** within the nanowells. At first, the chloroform-soluble *meso*-tetraphenyl-$\beta$,$\beta$-dihydroxychlorin (**B**) or **4** was deposited within the wells with a porphyrin (**A**) or **1b** bottom. The particles were filtered with a 100 nm steel frit in combination with a 200 nm pore filter. This was the most efficient combination in our hands, because we could not find any commercial filter with smaller pores and which was stable enough against chloroform. After redissolution in water, the ratio of the areas of the Soret band of the bottom porphyrinate **1b** at 420 nm and the chlorin band at 660 nm in the UV/vis spectra was about the same as that in a $10^{-6}$ molar ethanol solution of both components in a 1:1 ratio. Manganese(III) porphyrinate (**C**) or **1d** was then added, and the particles were centrifuged after 2 h. All three components **A**, **B**, and **C** were then detectable in UV/vis spectra of aqueous or chloroform solutions of the resuspended particles. The fluorescence spectrum (Figure 3a) showed only fluorescence of the bottom porphyrinate **A**; the chlorin's **C** fluorescence was completely quenched by the manganese porphyrinate **C**. The procedure was also inverted: first manganese porphyrinate **1d** or **B**, and then chlorin **4** or **C**. In this ordering, the chlorin fluorescence was quenched only to about 50%.

Several control experiments confirmed the fixation of both solutes within the nanowells:

(i) After ultrafiltration of the **1b** → **3a** → **4** (=**A**,**B**,**C**) particles, redissolution in chloroform or water, and removal of the particles by a second ultrafiltration, no chlorin was detectable in the supernatant by fluorescence measurements. Visible spectra showed no changes of relative absorption intensities of the dyes adsorbed to the silica particles.

(ii) When the first self-assembly step was carried out with the *meso*-[tetrabenzoyl chloride] porphyrin instead of the mixed anhydride, a large percentage of domains was formed. Titrations with the large manganese(III) porphyrin **1c** then produced up to 70% fluorescence quenching. If the manganese(III) porphyrins **3a** or **3b** were applied as quenchers in such a preparation, about 70% of the fluorescence was quenched within less than 10 s. This is another circumstantial proof that fitting of porphyrins within the nanowell is the only reason for the slowness and irreversibility of this attachment to the bottom of the nanowell.

(iii) The manganese(III) porphyrin **1d** (**A**) quenched 100% of the bottom porphyrin's fluorescence, but only 50% of the fluorescence of the chlorin **4** (**B**) above (Figure 3b). The corresponding copper(II)porphyrin **1f** (**B′**), however, quenched 100% of the fluorescence of both the bottom porphyrin and the chlorin above (Figure 3c). The chloride counterion of the manganese(III) central ion thus keeps the chlorin at a distance, whereas the ligand-free copper(II) gets close to both chromophores. The latter result suggests strongly that the nanowell contained only three dye molecules, not more.

The UV/vis spectra of silica particles with **A**,**B**,**C** (**1b**,**4**,**1d**) or **A**,**C**,**B** (**1b**,**1d**,**4**) ordering were practically indistinguishable (Figure 4). This indicates that within the limits of error only one molecule of **4** or **1d** was trapped in each individual nanowell. If, for example, the chlorin **4** was fixated at the bottom, no other molecule of **4** was bound to a measurable extent, although the estimated number of nanowells on the weighed-in particles (3.0 mg) was about 20−30 times smaller than the number of dissolved molecules ($\sim 2 \times 10^{16}$ molecules for $\sim(4-6) \times 10^{14}$ nanowells). A smaller excess did not lead to quantitative quenching, because many quencher molecules were presumably adsorbed at surfaces and washed off in the cleaning procedure (see Experimental Section). The observed occupation by only one molecule in each self-assembly procedure, which allowed sorting, may be caused by a cooperation of several effects: during the sorting process, the porphyrins stand most of the time upright (see Discussion, Figure 6) and

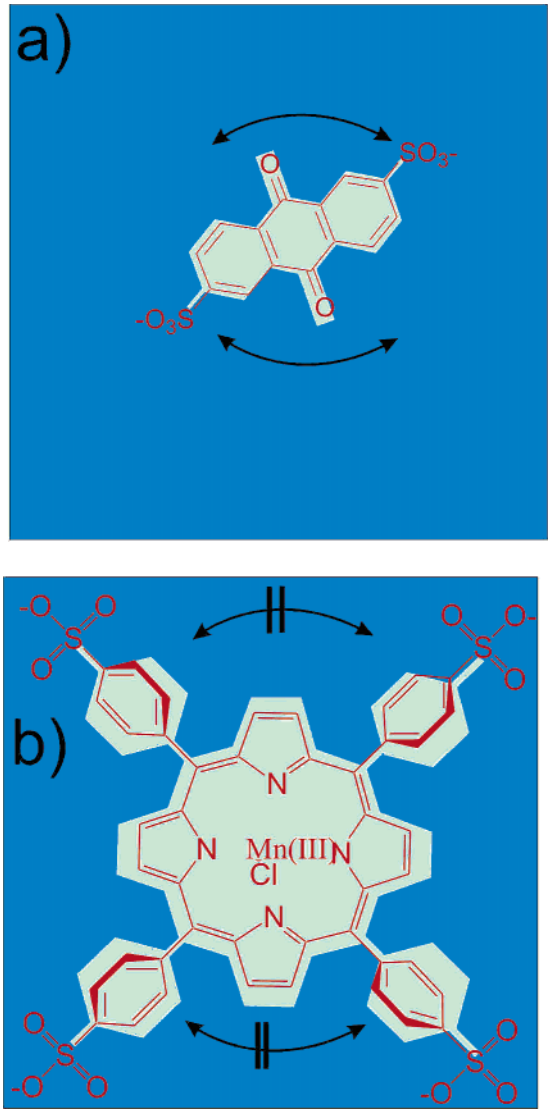


***Figure 6.*** Model of molecules (red) which are attached to hydrophobic walls (green) of the nanowells by van der Waals interactions: (a) small molecules and (b) molecules of the same size as the hydrophobic walls of the nanowells. The blue color indicates solvated (water, chloroform, etc.) parts of the walls; (a) is removed very quickly by solvents within the well, while (b) is removed only very slowly.

would not leave enough room in the nanowell for a second one to enter; the 10−20-fold excess may be adsorbed to a large part on the OEG-coated particles and may be washed off in the isolation procedure; the time period needed for the trapping of a second porphyrin is longer than the time allowed for self-assembly.

We also developed an independent electrochemical method to check the result of the ordering. The silicate particles were dissolved in the ethyl acetate solution of a silver colloid, and the solution was dropped on a gold electrode and dried. Probes with the manganese(III) porphyrin **1d** on top of the well (ordering: **1b** → **4** → **1d** or **A**,**B**,**C**) produced a reduction wave at −400 mV, and probes with the chlorin on top (ordering **1b** → **1d** → **4** or **A**,**C**,**B**) did not (Figure 5). The manganese(III) porphyrin presumably took up an electron from the electrode via Au-dispersed silver crystallites, which connected the surface of the particles with the electrode. The reduction occurred slowly, inefficiently, and irreversibly. It was, however, completely abolished, when the manganese(III) porphyrin was covered by the electrochemically inactive chlorin **4** molecule.

The nanowells were finally completely destroyed by solvents, which break the hydrogen bonds within their walls. DMSO or DMF, for example, immediately removed the entrapped molecules. Centrifugation, redissolution in pure water, a second centrifugation, and redissolution in water or chloroform/ethanol yielded particles with intact nanowells. They could again be packed with porphyrins and chlorines under the described conditions.

## Discussion

A special solution of Fick's second law (eq 1) was used to deduce "diffusion constants" from the experimental results (Figures 1 and 2), although the extremely slow reorientation within the 2 nm box certainly does not correspond to an equilibration of concentration gradients. It is essentially a slow rotation, which ends in a trapping by van der Waals interaction with the bottom porphyrin. The advantages of the applied diffusion formalism lie first in the dimension of the time-constant obtained, $m^2\ s^{-1}$ and not only $s^{-1}$, second in the possibility to visualize the slowness of the process by comparisons with known diffusion processes in bulk media and pores, and, most important, in the finding that eqs 1 and 2 reproduce several data sets correctly. Furthermore, it helps in the intuitive interpretations considering a solute−wall interaction (see Figure 6). A similar approach to describe the diffusion in a restricted geometry was applied for micellar reaction systems,[14] where the dissolved molecules can rotate freely within the micelles.

In our case, the diffusion process is clearly dominated by the fitting of solutes within the rigid nanowell. This is also related to the diffusion in pores, which has been evaluated by Pappenheimer's eq 3. Here, a coefficient $\lambda$ is defined, which is the ratio of the molecule-to-pore size.[12,15,16] $D$, the diffusion constant of the molecule in the pore, and $D_o$, the diffusion constant in bulk solution, are then empirically related as follows:

$$D/D_o = (1-\lambda)^2[1-2.1044\lambda + 2.0888\lambda^3 - 0.948\lambda^5] \quad (3)$$

For $\lambda = 1$, the molecule is exactly fitting the pore, and the equation predicts no diffusion at all and is not applicable. Nevertheless, the prediction is close to what we find for fitting molecules in nanowells, where fitting molecules diffuse 14 orders of magnitude slower than in solution. For $\lambda = 0.5$, the measured diffusion constants $D_o$ and $D$ of porphyrins differed by less than 2 orders of magnitude.[12] For the nanowells, it has been shown earlier that smaller anthraquinone molecules reach their bottom within the time limit of a few seconds of our detection method.[6] The same holds true for manganese(III) porphyrinates **3b**,**c**, which diffuse freely into larger nanowells with an extended bottom made of porphyrin domains. The

(9) Zachmann, H. G. *Mathematik für Chemiker*; Verlag Chemie: Weinheim, 1974.
(10) Shull, K. R.; Kramer, E. J.; Hadziioannou, G.; Antonietti, M.; Sillescu, H. *Macromolecules* **1988**, *21*, 2578−2580.
(11) Byers, G. W. *Macromolecules* **1993**, *26*, 4242−4248.
(12) Kathawalla, I. A.; Anderson, J. L.; Lindsey, J. S. *Macromolecules* **1989**, *22*, 1215−1219.
(13) (a) Sagiv, J. *Isr. J. Chem.* **1989**, *18*, 346−353. (b) Sagiv, J. *J. Am. Chem. Soc.* **1980**, *102*, 92−98.
(14) Hetlee, M. D.; Kozak, J. J.; Rothenberger, G.; Infelta, P. P.; Graetzel, M. *J. Phys. Chem.* **1980**, *84*, 1508−1519.
(15) Pappenheimer, J. R.; Renkin, E. M.; Borrero, L. M. *Am. J. Physiol.* **1951**, *167*, 13−21.
(16) Deen, W. M. *AIChE J.* **1987**, *33*, 1409−1412.

acceleration effect of different solvents is less than 10-fold. The finding that the diffusion process in ethanol or chloroform is only slightly faster than that in water shows that immobile "ice-structures" on the hydrophobic walls, as indicated by model studies[17] and as assumed earlier for the nanowells,[1−4] are not important. The observed small temperature effects (Figure 2c) indicate the same.

The description of the time-course by a time-constant with a dimension of $m^2\ s^{-1}$ or $m^3\ s^{-1}$ is satisfactory with respect to most of the data of Figures 1 and 2. The extremely slow 1-nm motion within the nanowell has, however, nothing in common with movements along random diffusion pathways. They are presumably dominated almost exclusively by interactions between the walls with porphyrin solutes of similar size. We assume that the diffusion into the nanowell is faster by a factor of at least $10^{10}$ than that of the rotations, which finally leads the solute into a position parallel to the bottom porphyrin. In all probability, the entering porphyrin molecule is at first strongly adsorbed by the hydrophobic walls and squeezes out most solvent molecules, which separate it from the hydrophobic wall. This is indicated by a green background in Figure 6b. The fitting molecule, directly glued on the wall by van der Waals interactions, is only slowly desorbed, because it cannot slide onto solvated parts of the wall, which are colored blue in Figure 6. Smaller quencher molecules such as anthraquinone disulfonate or the same molecule on a larger wall, for example, manganese porphyrinate **1d**, above a domain of two or more bottom porphyrins are adsorbed in the same manner, but they separate quickly into the solvent, because it can diffuse freely onto neighboring solvated parts of the wall (Figure 6) and is desorbed. A slow desorption process of molecules, which fit in size to the walls of a nanocube, has, to the best of our knowledge, never been evaluated. It should follow the same $t_{1/2}-l^2$ or possibly $t_{1/2}-l^3$ relationships, which have also been found in simulations of our experimental curves.

The movement of the fitting porphyrins into the nanowells drives them irresistibly to the bottom, where they then stay permanently as long as the nanowell's shape does not change. The stronger binding to the porphyrin bottom as compared to the alkane walls should be caused first by the open edge at the top of the walls and by the unique rigidity of the porphyrin moiety, which leads to strictly parallel adjustments. It is exclusively this removal from the equilibrium which makes the enrichment and entrapment of the porphyrins in the negligibly small volume of the nanowells possible. The monomolecular trapping from a dilute bulk solution ends in stacks of three single molecules, which would be perfectly soluble in a less restricted environment. The observation that the Mn−Cl porphyrin **1d** quenches the fluorescence of the bottom porphyrin quantitatively indicatess that the chloride ions are pushed out of the space between the bottom and the adsorbed porphyrins together with the solvent molecules. This was not reversed by chlorin **4**. It is therefore separated selectively by the chloride counterion from manganese and only weakly quenched. A solvent-free dimer is thus finally formed on the well's bottom. Phenyl−phenyl repulsion should then enforce a rotation of the upper monomer by 45° against the bottom porphyrin. The diameter of the nanowell, which limits the access of porphyrins, is therefore not equal to the side-length of the square (2.2 nm), but to the length of its diagonal (2.8 nm). This explains why the *p*-tetrasulfonate **1d** reaches the nanowell's bottom: it orients its phenyl substituents in the direction of the diagonal. The third component of the stack should then have the same orientation as the bottom porphyrin (Figure 7). Once the solvent molecules are squeezed out of the bottom of the nanowell and the porphyrins are in close contact, the adsorption process becomes irreversible as long as the nanowells above are intact. The mobility of both solvents and solutes is too restricted to overcome the van der Waals forces.

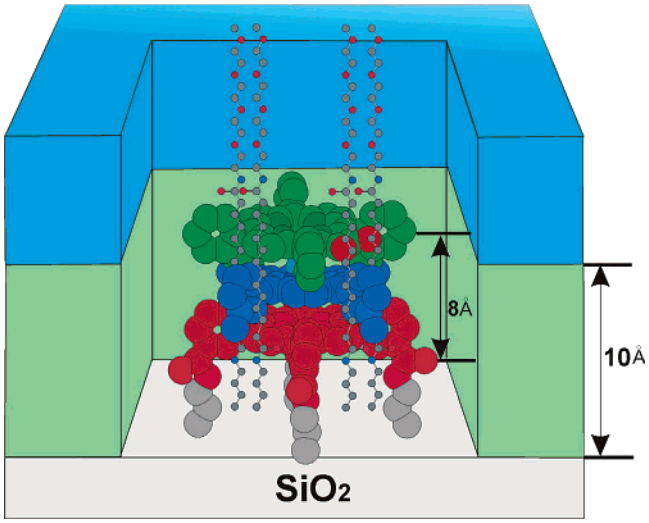


***Figure 7.*** Model of the stacking of three phenyl porphyrins **1b**, **1e**, and **4** (**A**,**B**,**C**) at an angle of 45° in a 2 nm nanowell.

Sorting depends not only on the apparent irreversibility of the final adsorption process, but also on the limitation to only one molecule in each nanowell at a time. This limitation was not achieved by establishing a 1:1 ratio between the number of nanowells and accessible porphyrins in aqueous or chloroform solutions. An at least 10-fold excess was needed to quench the fluorescence of all bottom porphyrins in the first loading procedure. This excess could have filled the nanowells completely with two or three of the quencher molecules, but this was never observed. The Soret band ratio between **1b** (420 nm) and manganese complex **1d** (470 nm) was always found to correspond to a ratio of 1:1, and the same was found for **1b** and chlorin **4** (650 nm). These relative absorption measurements of colored colloidal particles had a large limit of error (about ±10% for Mn(III) and ±20% for the chlorin), but were perfectly reproducible within these limits. We never found evidence for significant overloading even after several hours. We believe that the 10-fold excess of solute molecules is adsorbed on the outer surface of the particles or on the walls of the cuvettes and is later removed quantitatively in the filtration, centrifugation, and washing procedures. Successful sorting thus primarily depends on the fitting of molecules and reliable analytic methods for the sorted stack, in particular, fluorescence measurements. We believe, however, that our protocol will also allow the introduction of colorless steroids, alkaloids, and fullerenes as spacers and of almost colorless quinone-type compounds as electron acceptors. The analysis of such molecular stacks will then depend on indirect methods, in particular, shielding of the bottom porphyrin from small fluorescence quenching molecules and investigation of charge separation between the bottom and top components by flash photolysis. Heterodimers with the

(17) Vossen, M.; Forstmann, F. *J. Chem. Phys.* **1994**, *101*, 2379−2390.

desired distances for charge separation between 6 and 12 Å will thus become accessible and should be easy to optimize in series. Furthermore, it should be possible to repair bleached noncovalent systems. Adsorbed components can be removed by the dissolution of the particles in water or solvents containing 10% DMF. Centrifugation and reorganization in water or chloroform/ethanol then recovers active particles. A fourth component can also be fixed at a larger distance by attaching it to an ammonium ring at the well's rim.[2,6]

The nanowell system is thus promising in many respects, but it appears to have two serious limitations in its present form:

(i) The 2-nm width of the nanowells is not ideal. To produce functional systems, one has to synthesize conductors, distance holders, and electron acceptors of this exceptional width, which is not necessary with respect to functionality. Nature uses 1-nm-sized protoporphyrin and chlorophyll derivatives as electron donors and even smaller amino acids and quinones as acceptors. One-nanometer nanowells with a bottom made of similar protoporphyrin- or chlorophyll-type dyes would allow the direct application of a large variety of commercially available, redox-active compounds in sorted stacks. Work along this line is in progress.

(ii) The system relies on smooth surfaces, which automatically limits the number of nanowells on the surface of a given volume of carrier material. Catalytic and energy-converting systems should therefore be spread rather on planar thin layers similar to leaves instead of bulky spheres. We have been successful in the development of planar gold colloids,[5] but could not produce any nonmetallic colloidal leaflets so far. Several years ago, however, we obtained electron micrographs of insoluble D,L-polylysine $\beta$-pleated sheets made simply by mixing soluble D- and L-helices.[18,19] Such lysine sheets or similar polyfunctional polymer sheets may be solubilized with a monolayer of bolaamphiphiles **2**, and nanowells may be established on both sides of such ultrathin sheets. This approach is currently being investigated.

**Acknowledgment.** Financial support by the Deutsche Forschungsgemeinschaft (SFB 348 "Mesoscopic Systems", Graduiertenkolleg "Hydrogen Bonds"), the European TMR research network "Carbohydrate Recognition of Nucleic Acids (Carbona)", the Fonds der Deutschen Chemischen Industrie, and the FNK of the Free University is gratefully acknowledged.

**Supporting Information Available:** The derivation and application of eqs 1 and 2. This material is available free of charge via the Internet at http://pubs.acs.org.

JA048310V

(18) Fuhrhop, J.-H.; Krull, M.; Bueldt, G. *Angew. Chem., Int. Ed. Engl*. **1987**, *26*, 699−700.
(19) Dzwolak, W.; Ravindra, R.; Nicolini, C.; Jansen, R.; Winter, R. *J. Am. Chem. Soc.* **2004**, *126*, 3762−3768.